Available online at www.sciencedirect.com

ScienceDirect

www.journals.elsevier.com/journal-of-environmental-sciences

JOURNAL OF ENVIRONMENTAL SCIENCES
www.jesc.ac.cn

Effect of $AlCl_3$ concentration on nanoparticle removal by coagulation

Lizhu Zhang[1,*], *Jingchun Mao*[1], *Qing Zhao*[2,*], *Shaobo He*[1], *Jun Ma*[3,*]

1. *Chemistry Department of Science School, Harbin Institute of Technology, Harbin 150090, China*
2. *Institute of Applied Ecology, Chinese Academy of Sciences, Shenyang 110016, China*
3. *School of Municipal and Environmental Engineering, Harbin Institute of Technology, Harbin 150090, China*

ARTICLE INFO

Article history:
Received 28 February 2015
Revised 15 April 2015
Accepted 17 April 2015
Available online 4 July 2015

Keywords:
Nanoparticles
Coagulation
Effective coagulation concentration
Al^{3+}

ABSTRACT

In recent years, engineered nanoparticles, as a new group of contaminants emerging in natural water, have been given more attention. In order to understand the behavior of nanoparticles in the conventional water treatment process, three kinds of nanoparticle suspensions, namely multi-walled carbon nanotube-humic acid (MWCNT-HA), multi-walled carbon nanotube-N,N-dimethylformamide (MWCNT-DMF) and nanoTiO_2-humic acid (TiO_2-HA) were employed to investigate their coagulation removal efficiencies with varying aluminum chloride ($AlCl_3$) concentrations. Results showed that nanoparticle removal rate curves had a reverse "U" shape with increasing concentration of aluminum ion (Al^{3+}). More than 90% of nanoparticles could be effectively removed by an appropriate Al^{3+} concentration. At higher Al^{3+} concentration, nanoparticles would be restabilized. The hydrodynamic particle size of nanoparticles was found to be the crucial factor influencing the effective concentration range (ECR) of Al^{3+} for nanoparticle removal. The ECR of Al^{3+} followed the order MWCNT-DMF > MWCNT-HA > TiO_2-HA, which is the reverse of the nanoparticle size trend. At a given concentration, smaller nanoparticles carry more surface charges, and thus consume more coagulants for neutralization. Therefore, over-saturation occurred at relatively higher Al^{3+} concentration and a wider ECR was obtained. The ECR became broader with increasing pH because of the smaller hydrodynamic particle size of nanoparticles at higher pH values. A high ionic strength of NaCl can also widen the ECR due to its strong potential to compress the electric double layer. It was concluded that it is important to adjust the dose of Al^{3+} in the ECR for nanoparticle removal in water treatment.

Introduction

Nowadays, engineered nanoparticles (ENPs) have attracted a great deal of attention because of their increasing production and use (Luan and Tan, 1992). As the use of ENPs continues growing rapidly, it is inevitable that these particles will enter natural aquatic systems if they are not properly controlled during their production, use and disposal. Recent studies on the toxicity of nanoparticles showed that nanoparticles may pose a risk to human health and organisms in aqueous systems if present at sufficiently high concentrations (Lin et al., 2010). Thus finding a proper method to remove ENPs from water is urgently needed.

Coagulation has been widely used to remove suspended matter and some colloid matter in water treatment (Gurusamy

* *Corresponding authors.*
E-mail addresses: zlz4513@sina.com (Lizhu Zhang), zhaoqing@iae.ac.cn (Qing Zhao), majun@hit.edu.cn (Jun Ma).

http://dx.doi.org/10.1016/j.jes.2015.04.014
1001-0742/

Annadurai and Lee, 2004). Studies on potable water treatment unit processes (especially coagulation) related to ENP removal have suggested that there are many factors influencing the removal efficiency for nanoparticles. Reijnders (2006) suggested that standard wastewater treatment may be ineffective in the removal of nanomaterials, whereas Wiesner et al. (2006) concluded that the involvement of nanomaterials in current water treatment systems may not become a problem. Meanwhile, Zhang et al. (2008) reported that coagulation removal efficiencies of selected metal oxide nanoparticles ranged between 20% and 60% and Holbrook et al. (submitted for publication) confirmed that multi-walled carbon nanotubes (MWCNTs) could be removed from the aqueous phase *via* coagulation using either ferric chloride or aluminum sulfate (alum). Liu et al. (2012) investigated the removal of dispersant-stabilized carbon nanotube (CNT) suspensions and concluded that the removal efficiency of these particles was dependent on dispersant type, coagulant type and coagulant dosage. Also, Hyung and Kim (2009) found that the removal of nC_{60} depended on coagulant dose.

The above studies showed that the ENP coagulation removal efficiency is closely related to the coagulant type and dosage. In our previous research (Zhang et al., 2014), we found that the $AlCl_3$ dosage can transform the electric charge of C_{60} from a negative to positive charge and re-stabilize the particles in suspension. We believe that the coagulant dosage can significantly affect the stability of nanoparticles by varying their surface charges. As the surface charge carried by nanoparticles is related to their type and size, it is necessary to investigate the variation of the effective concentration range (ECR) of Al^{3+} with the type and size of nanoparticles, which would benefit the manipulation of the coagulant to obtain effective removal of nanoparticle by coagulation in actual water treatment. Therefore, two kinds of nanoparticles, CNT and TiO_2 were dispersed in humic acid (HA) and N,N-dimethylformamide (DMF) to prepare three suspensions with different particle sizes, CNT-HA, CNT-DMF and TiO_2-HA, to investigate how their removal efficiency varied with the dosage of Al^{3+}, and the variation of the ECR of Al^{3+} with nanoparticle size was explored.

1. Materials and methods

1.1. Nanoparticles

Multi-walled CNTs were purchased from Nanotech Port Co., Shenzhen, China (Model CN3016). Before their use, CNTs were dispersed into a 150 mL flask containing 40 mL concentrated acid solution (30 mL HNO_3, 10 mL H_2SO_4) for 24 hr to remove residual metal catalyst. Then, CNTs were washed by deionized water. Finally, the CNT-containing solution was filtered by a 0.45 mm glass-fiber filter and dried at 80°C in a hot air oven overnight to obtain purified CNTs. TiO_2 (25 nm) was purchased from Sigma-Aldrich. Aldrich HA was purified according to a previous study (Pan et al., 2006). Briefly, 0.1 mol/L NaOH and 0.1 mol/L $Na_4P_2O_7$ were mixed with Aldrich HA (50:1, *V*/*W*) to extract the HA. The supernatants were filtered and collected. The supernatants were then precipitated by HCl. The precipitated HAs were washed using distilled water until a chloride test using $AgNO_3$ was negative for chloride, freeze-dried and ground to <500 μm particles. The purified HAs were then dissolved into deionized water and adjusted to pH 12 with 0.5 mol/L NaOH. After 10 hr stirring, the solution was filtered through a 0.20 μm cellulose acetate membrane filter and stored at 4°C. The concentration of HA in the filtrate was 525 mg/L quantified by total organic carbon (TOC). DMF was purchased from Tianjin BODI Company, China.

1.2. Carbon nanotube and TiO_2 suspensions

HA and DMF were used as dispersants to prepare MWCNT-HA, MWCNT-DMF and TiO_2-HA suspensions. 50 mg of nanoparticles was dispersed into 25 mL HA solution (525 mg/L) and pure DMF solvent, respectively. The mixture was shaken for 12 hr at 25°C in a thermostat oscillator. Then, the mixture was poured into 750 mL super pure water. After that, the pH of the mixture was adjusted to 10.0 with 0.1 mol/L NaOH. The suspension was then sonicated for 1.5 hr at 40 KHz with an intensity of 150 W/L (2000U, Ultrasonic Power Co, China) and stored at 25 ± 2°C for no longer than 10 hr before its use.

1.3. Coagulation experiments

A jar test was used to evaluate the removal efficiency of nanoparticles by the coagulation process in a Jar Mixer (Tianjin, China) with six paddles. 250 mL water samples containing nanoparticles were used in the experiments and their characteristics are shown in Table 1. $AlCl_3$ was used as coagulant. The jar tests were performed in three steps: (1) rapid mixing for 2 min at 200 r/min, (2) slow mixing for 20 min at 100 r/min, and (3) settling for 30 min. After the settling step, the supernatants at 1 cm below the surface were extracted for measurement.

1.4. Analytical methods

The size of nanoparticles was analyzed by dynamic light scattering (DLS) using a Zetasizer (Zetasizer ZS90, Bedford Co, MA, USA) equipped with a folded capillary cell at 25°C. The zeta potential was analyzed using a Zeta 90 Plus Zeta Potential Analyzer (Brookhaven Instruments Co., Holtsville, NY, USA). The initial concentration of CNT in the suspensions was quantified by TOC (TOC-5000, Daojin Co., Japan) with subtraction of the TOC of the dispersant. The quantification of TiO_2 was measured by an Inductively Coupled Plasma Atomic Emission Spectrometer (ICP) (Optima 7300, Perkin Elmer Co, MA, USA). Briefly, 3.0 mL of the TiO_2 suspension was collected in a test-tube and 2.0 mL pure HF was added. Then the tube was heated at 155°C 1 hr. After that, 1.0 mL pure $HClO_4$ was added into the tube and heating was continued at 165°C until the liquid volume was about 1 mL. In this process, the tube cap should not be fastened tightly to let the vapor escape. The resulting liquid was diluted by HNO_3 solution (2.0%) according to its concentration. Finally, the sample was used for measurement by ICP.

The turbidity was used to quantify the removal efficiency of MWCNT and TiO_2 by the formula (1-Turbidity end) /Turbidity initial × 100% after coagulation. All samples were run in duplicate.

Table 1 – Characteristics of nanoparticles.

NP	(mg/L)	Dispersant (mg/L)	DLS particle size (nm)	Zeta potential (mV)	Stability (%)
MWCNTs	12.5	HA/17.5	299.0 ± 1.0	−34.7 ± 2.3	50.18 ± 0.5
TiO_2	12.03	HA/17.5	321.1 ± 1.3	−30.4 ± 3.1	46.5 ± 0.8
MWCNTs	11.5	DMF/5.0	190.0 ± 1.8	−37.9 ± 2.7	54.18 ± 0.2

NP: nanoparticle; MWCNTs: multi-walled carbon nanotubes; HA: humic acid; DMF: N,N-dimethylformamide; DLS: dynamic light scattering. Stability was calculated by formula: $(C_0 - C_t)/C_0 \times 100\%$ (C_0 is the initial concentration of nanoparticles in the suspension, C_t is the concentration of nanoparticles in suspension measured after 24 hr settlement at pH 7.0).

2. Results and discussion

2.1. Characteristics of nanoparticles

The nanoparticles were aggregated in aqueous solution. The hydrodynamic particle size of the nanoparticles (Table 1) was much greater than the labeled value (<50 nm). MWCNTs were better dispersed in DMF (190.0 nm) than in HA (299.0 nm) indicating that the dispersant affected the hydrodynamic particle size of the nanoparticles. A suspension with smaller particles is more stable. The particle size of nanoparticles followed the order MWCNT-DMF < MWCNT-HA < TiO_2-HA, while the stability of the suspension followed the reverse order MWCNT-DMF > MWCNT-HA > TiO_2-HA. All nanoparticles carried negative charge and their zeta potentials were lower than −30 mV.

2.2. Removal rate of nanoparticles by coagulation

All removal rate curves appeared as a reverse "U" type and could be divided into three zones with increasing $AlCl_3$ concentration (Fig. 1) (Luan and Tan, 1992). (1) "no significant removal zone", where the removal rate remained low. The low dosage of Al^{3+} is insufficient to cause the destabilization of nanoparticles; (2) "effective coagulation zone (ECR)", where the removal rate sharply increased and reached a plateau. For MWCNT-HA, MWCNT-DMF and TiO_2-HA suspension, the ECR of Al^{3+} was 0.05–0.4 mmol/L, 0.05–3.5 mmol/L and 0.1–0.4 mmol/L respectively. The nanoparticle removal rate can be higher than 90% in the ECR by exclusion of the endpoint; and (3) "re-stabilization zone", where the removal rate decreased due to the re-stabilization of precipitated nanoparticles.

Four mechanisms are generally described to regulate colloid removal by coagulants, which are electric double layer compression, adsorption charge neutralization, inter-colloid bridging, and sediment netting/sweep coagulation (Ahmad et al., 2006). Liu et al. (2012) considered that the major mechanism for the removal of dispersant-nanoparticles by alum could be charge neutralization. The positively-charged hydrolysis product of alum could strongly adsorb to the negatively-charged nanoparticles, and subsequently, neutralize the surface charges of the nanoparticles, diminish the electrostatic repulsion between them, and then precipitate the stabilized-nanoparticles. However, alum could over-saturate the negatively-charged nanoparticle surfaces and make the surfaces reversely-charged (zeta potential changes from negative to positive) at a high concentration, which may then re-stabilize the nanoparticles due to the reproduced electrostatic repulsion between particles. Re-stabilization of coagulated colloids originating from the oversaturation of polyelectrolytes has been reported by Pinotti and Zaritzky (2001).

The breadth of the ECR appears similar for MWCNT-HA and TiO_2-HA, indicating that the ECR is related to the dispersant used to disperse nanoparticles. Liu et al. (2012) also found the

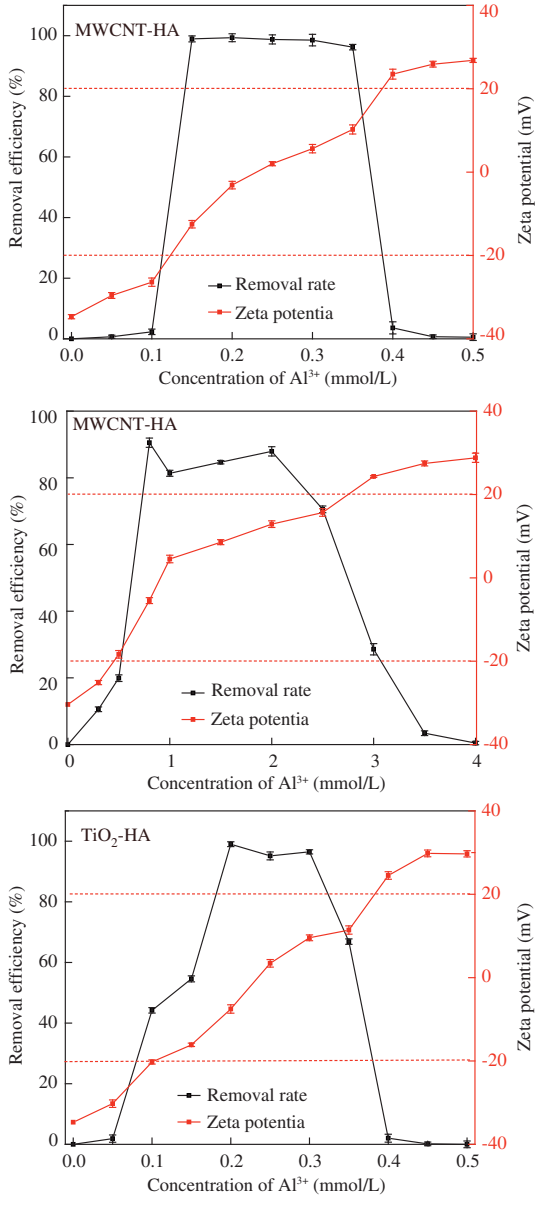

Fig. 1 – Removal rate and zeta potential of nanoparticles varied with the dosage of Al^{3+}.

ECR varied with the dispersant used to disperse nanoparticles when they used poly aluminum chloride to coagulate CNT dispersed by five kinds of dispersants. According to the characteristics of nanoparticles (Table 1) caused by the dispersant, it was inferred that the particle size of nanoparticles was the crucial factor influencing the ECR. A smaller particle size tends to cause a broader ECR. Thus the particle size of the three suspensions followed the order MWCNT-DMF < MWCNT-HA < TiO_2-HA, while the width of the ECR followed the reverse order. Nanoparticles were destabilized in the range of zeta potential varying nearly from −20 to + 20 mV in the corresponding ECR. With increasing dose of $AlCl_3$, nanoparticles will be restabilized again.

For a well-dispersed nanoparticle suspension, a large proportion of small size nanoparticles existed in the suspension that carried more negative charges compared to larger size particles. Such a suspension will consume more alum to neutralize their negative charges and induce them to destabilize in the process of coagulation. For example, the addition of 0.05 and 0.1 mmol/L Al^{3+} will cause the zeta potentials of MWCNT-HA (299.0 nm) and TiO_2-HA (321.1 nm) to increase from −30 to −20 mV, respectively. A dose of 0.4 mmol/L Al^{3+}

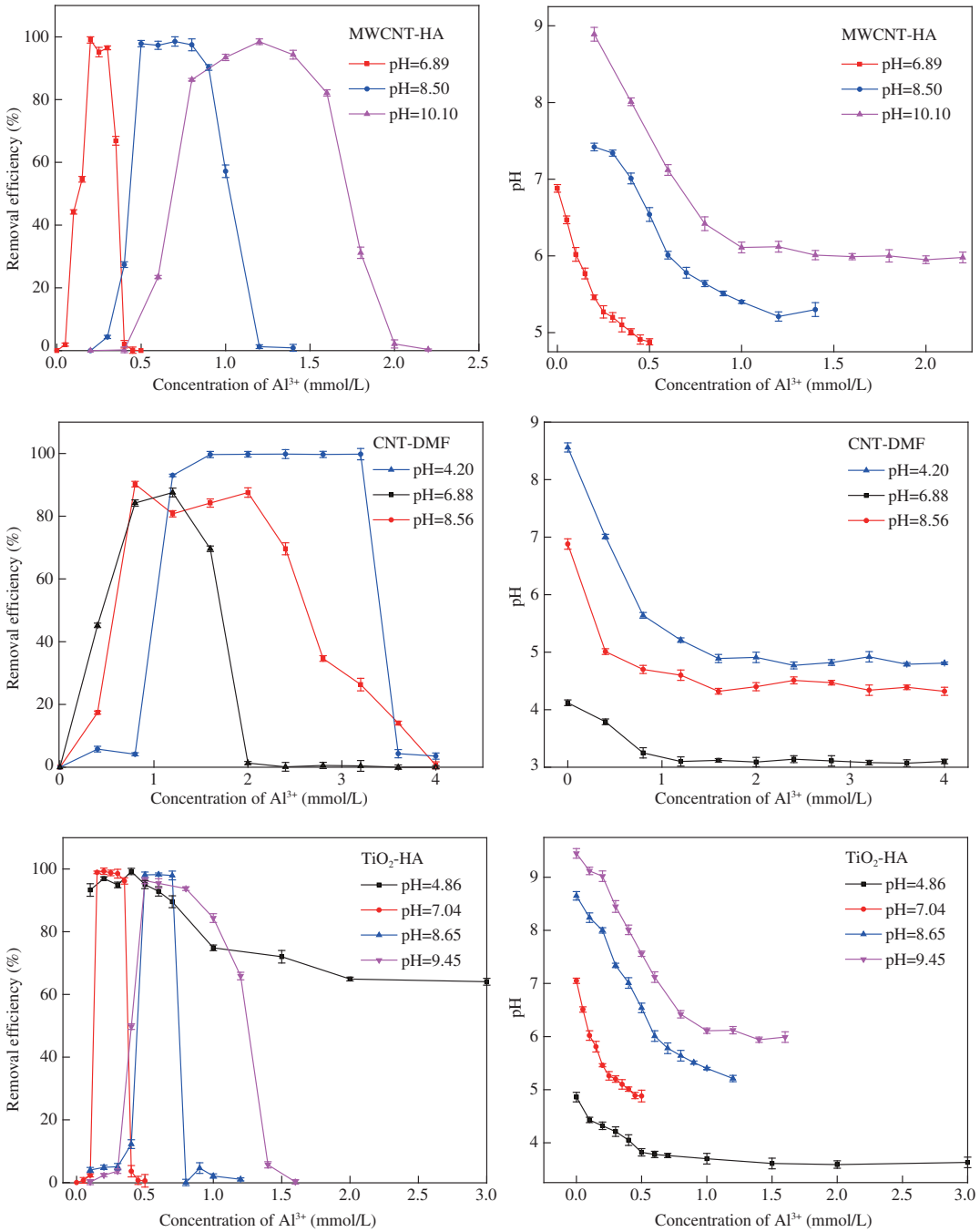

Fig. 2 – Changes of effective concentration range (ECR) of Al^{3+} at different pH. The left figures showed ECR in acid condition, neutral condition and basic condition, pH was measured after coagulation.

will cause the zeta potentials to increase to higher than +20 mV, while the dose of Al^{3+} should be 0.6 mmol/L to change the zeta potential of MWCNT-DMF (190.0 nm) from –30 to –20 mV. The addition of Al^{3+} at 3.5 mmol/L will increase the zeta potentials to higher than +20 mV. Therefore, oversaturation was achieved at a higher concentration of Al^{3+}, and a relatively larger ECR was obtained for smaller size nanoparticle suspensions.

2.3. Effect of pH on ECR

Consistent with the reported results (Amuda and Amoo, 2007), initial pH had an important effect on the coagulation behavior of the Al-based coagulants and was investigated for its effect on the nanoparticle removal rate. The final pH after coagulation at each dose of Al^{3+} was also determined.

All the removal curves appeared to have a reverse "U" shape at different pH, except for the TiO_2-HA suspension at pH 4.86. The ECR became broader and the removal curves moved to the right with increasing pH. For example, the ECR of the MWCNT-HA suspension was 0.1–0.4 mmol/L, 0.3–1.2 mmol/L and 0.4–2.0 mmol/L at pH 6.89, 8.50 and 10.10 respectively (Fig. 2). For MWCNT-DMF, the ECR was 0.0–2.0 mmol/L, 0.0–4.0 mmol/L and 0.8–3.6 mmol/L at pH 4.20, 6.88 and 8.56; while for TiO_2-HA, the ECR was 0.1–0.4 mmol/L, 0.4–0.8 mmol/L and 0.4–1.4 mmol/L at pH 7.04, 8.65 and 9.45 respectively. The special ECR shape of TiO_2-HA at pH 4.86 was probably attributable to the instability of TiO_2 nanoparticles in acid conditions. The hydrodynamic particle size of TiO_2-HA was almost 500 nm at pH 4.86 even in the absence of $AlCl_3$ (shown in Appendix A Fig. S1), which resulted in auto-precipitation. Compared with the three suspensions at similar pH, the breadth of ECR followed the order MWCNT-DMF > MWCNT-HA > TiO_2-HA, which is in accordance with the reverse order of particle size. The results further confirmed that the smaller nanoparticles induced a wider ECR regardless of the pH condition.

The effect of pH on ECR can be explained by the stability of the nanoparticle suspension and the hydrolysis product of alum. Previous studies (Dermontbouchard et al., 2009; Badawy et al., 2010) showed that nanoparticles tend to aggregate in acid conditions. In our study, the hydrodynamic particle size of nanoparticles was measured under different pH. The hydrodynamic particle size of nanoparticles is smaller in basic conditions than in acid conditions, which is consistent with previous studies. In acid conditions, dissociated acidic functional groups (hydroxyl, carboxyl and *et al.*) of nanoparticles may associate with hydrogen ions and reduce the repulsive interaction among nanoparticles. Consequently, the particles tend to aggregate and cause a relatively large particle size. However in basic conditions, the negative hydroxide ions lead the negative nanoparticles to be apart from each other. Therefore, these particles are well dispersed and have smaller size. Since smaller nanoparticles will consume more alum to neutralize their negative charges and induce them to destabilize in the process of coagulation, the ECR became broader and the removal curves moved to the right with increasing pH.

The coagulant hydrolyzed during the process of coagulation, which caused the pH to decrease as shown in Fig. 2. The hydrolysis products of Al^{3+} vary with the aqueous pH. The main hydrolysis reactions of coagulant are shown in Reactions (1)–(5) (Sparks, 2003)

$$[Al(H_2O)_6]^{3+} + H_2O \leftrightarrow [Al(OH)(H_2O)_5]^{2+} + H_3O^+ \quad (1)$$

$$[Al(OH)(H_2O)_5]^{2+} + H_2O \leftrightarrow [Al(OH)_2(H_2O)_4]^{+} + H_3O^+ \quad (2)$$

$$[Al(OH)_2(H_2O)_4]^{+} + H_2O \leftrightarrow [Al(OH)_3(H_2O)_3] + H_3O^+ \quad (3)$$

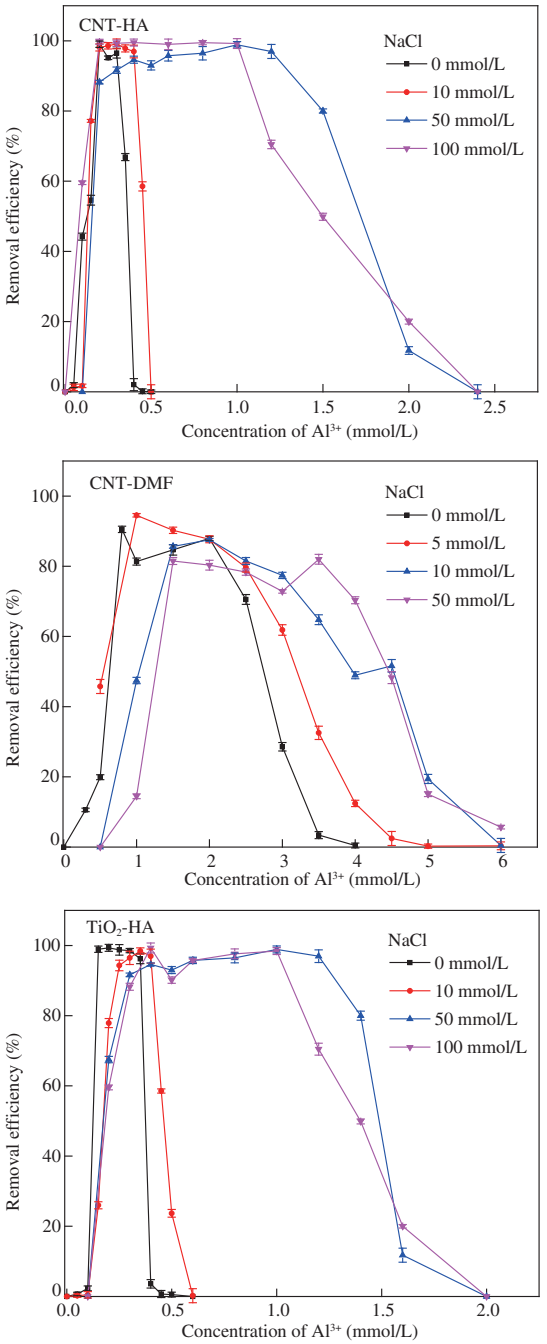

Fig. 3 – Effect of ionic strength on nanoparticle coagulation removal, pH = 7 ± 0.1. The ECR becomes broader with increasing ionic strength of NaCl.

$$[Al(OH)_3(H_2O)_3] + H_2O \leftrightarrow [Al(OH)_4(H_2O)_2]^- + H_3O^+ \quad (4)$$

$$xAl^{3+} + yH_2O \rightarrow Al_x(OH)_y^{(3x-y)+} + yH^+ \quad (5)$$

where, $Al_x(OH)_y^{(3x-y)+}$ represents positively charged Al-OH polymers, such as $Al_7(OH)_{17}^{4+}$, $Al_{13}(OH)_{34}^{5+}$, $[Al_{24}(OH)_{60}]^{12+}$, and $[Al_{54}(OH)_{144}]^{18+}$.

Cationic monomeric species of Al^{3+} and $Al(OH)^{2+}$ that have strong neutralization capability predominate at low initial pH (2 to 4). In addition, nanoparticles aggregate and form large size particles in this pH range. Therefore, a small amount of alum may over-saturate the negative charge of nanoparticles and re-stabilize them. Hence, a narrow ECR was found in this pH range. At initial pH 5 to 8, various monomeric species and polymeric species, such as $Al(OH)^{2+}$, $Al_6(OH)_{15}^{3+}$, $Al_7(OH)_{17}^{4+}$, $Al_{13}(OH)_{34}^{5+}$ will form (Merzouk et al., 2009; Can et al., 2002, 2006), which are the most effective alum species for nanoparticle destabilization because they carry more positive charges. However, nanoparticles become more stable in this pH range and exist in smaller sizes, carrying more negative charges. Therefore, these nanoparticles need more alum to neutralize their negative charges and over-saturate. Consequently, a wider ECR was obtained in this pH range. When the initial pH is higher than 9, the dominant species of alum is the monomeric $Al(OH)_4^-$ anion, which actually cannot be adsorbed by negative nanoparticles. However, the hydrolysis reaction of Al^{3+} will cause the final pH to decrease to lower than 9 (Fig. 2). Therefore, a positively charged hydrolysis product of alum can form and result in higher removal efficiency of nanoparticles in a wider ECR at this pH value.

2.4. *Effect of ionic strength*

In all cases, the ECR became wider with increasing the ionic strength of NaCl. For example, the ECR varied from 0.1–0.4 mmol/L to 0.1–2.4 mmol/L for MWCNT-HA and 0.1–0.4 mmol/L to 0.1–2.0 mmol/L for the TiO_2-HA suspension with the ionic strength of NaCl increasing from 0 to 100 mmol/L (Fig. 3). The ECR reached a plateau when the concentration of NaCl was higher than 50 mmol/L. For the MWCNT-DMF suspension, the ECR varied from 0–3.5 mmol/L to 0.5–6.0 mmol/L as the concentration of NaCl increased from 0 mmol/L to 50 mmol/L. The ECR of MWCNT-DMF reached a plateau at the concentration of NaCl of 10 mmol/L. The effect of ionic strength on ECR can be illustrated by the schematic model (Fig. 4).

The destabilization of nanoparticles caused by Al^{3+} can be described by the following steps. First, Al^{3+} hydrolyzed when it was added to the nanoparticle suspension (Step 1). Then the hydrolysis product of aluminum adsorbed to the surface of nanoparticles and caused the zeta potential of the nanoparticles to increase (Step 2). When the nanoparticles' zeta potential was higher than −20 mV, the nanoparticles started to destabilize. With increasing dose of Al^{3+}, the zeta potential of nanoparticles may change from negative to positive. In the range of zeta potential between −20 to 20 mV, nanoparticles can be destabilized and can be effectively removed (Fig. 1). Correspondingly the ECR of Al^{3+} was obtained. As the dose of Al^{3+} continued to increase, the zeta potential of nanoparticles increased to higher than

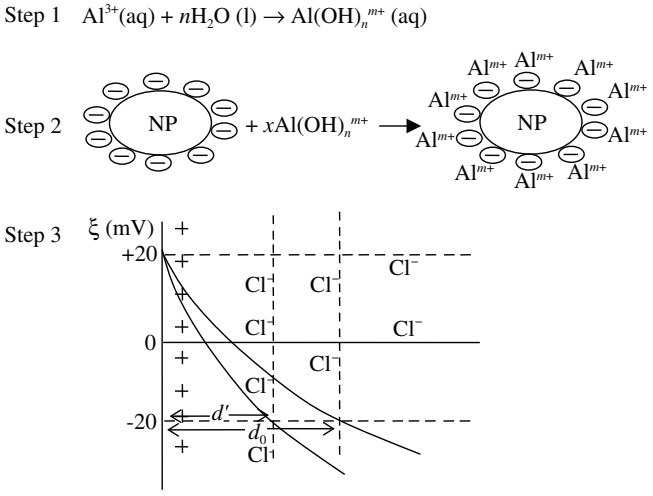

Fig. 4 – Schematic model of the effect of ionic strength on nanoparticle coagulation.

+20 mV. Nanoparticles were then re-stabilized, which resulted in lower removal efficiency. In the presence of NaCl, the higher ionic strength can compress the electric double layer of nanoparticles, making it thinner (from d_0 to d' in Step 3). The re-stabilized nanoparticles were then destabilized, which caused nanoparticles to be removed successfully even when the ECR of Al^{3+} was exceeded. Therefore, the ECR was widened with increasing ionic strength of NaCl. For the CNT-DMF suspension, the particle size is smaller and the particles more easily get closer together under the function of double layer compression. Therefore, a relatively lower ionic strength of NaCl could destabilize them. The ECR of Al^{3+} thus reached a plateau at lower concentration of NaCl. For MWCNT-HA and TiO_2-HA suspensions, however, the greater size of nanoparticles inhibits them from close access. Stronger compression of the electric double layer was needed to destabilize them. Therefore, higher ionic strength of NaCl was required to destabilize them and ECR reached the plateau at a relatively higher concentration of NaCl.

3. Conclusions

(1) Nanoparticle removal rate curves appeared to have a reverse "U" shape against Al^{3+} concentration. The ECR of Al^{3+} for CNT-HA, CNT-DMF and TiO_2-HA removal was 0.05–0.4 mmol/L, 0.05–3.5 mmol/L and 0.1–0.4 mmol/L respectively. With the appropriate concentration of Al^{3+}, the nanoparticle removal rate could be higher than 90%.

(2) The particle size is a crucial factor influencing the width of the ECR. Smaller size nanoparticles result in a wider ECR. With increasing pH, the ECR becomes broader, which can be explained by the small particle size of nanoparticles at higher pH value.

(3) Enhancing the ionic strength of NaCl can widen the ECR of coagulants because of its stronger capacity to compress the electric double layer of nanoparticles. The regenerated ECR of smaller size nanoparticles reached a plateau under relatively lower ionic strength compared

with bigger size particles. Optimization of conditions (pH, ionic strength *et al.*) to obtain the highest removal efficiency of nanoparticles by coagulants is required in future research.

Acknowledgements

This work was in part supported by the Hundreds Talents Program of Chinese Academy of Sciences, Open Foundation of State Key Laboratory of Environmental Criteria and Risk Assessment, Chinese Research Academy of Environmental Sciences (SKLECRA2015OFP10) and Natural Science Foundation of Heilong Jiang Province.

Appendix A. Supplementary data

Supplementary data associated with this article can be found in online version at http://dx.doi.org/10.1016/j.jes.2015.04.014.

REFERENCES

Ahmad, A.L., Sumathi, S., Hameed, B.H., 2006. Coagulation of residue oil and suspended solid in palm oil mill effluent by chitosan, alum and PAC. Chem. Eng. J. 118 (1-2), 99–105.

Amuda, O.S., Amoo, I.A., 2007. Coagulation/flocculation process and sludge conditioning in beverage industrial wastewater treatment. J. Hazard. Mater. 141, 778–783.

Badawy, A.M.E., Luxton, T.P., Silva, R.G., Scheckel, K.G., Suidan, M.T., Tolaymat, T.M., 2010. Impact of environmental conditions (pH, ionic strength, and electrolyte type) on the surface charge and aggregation of silver nanoparticles suspensions. Environ. Sci. Technol. 44, 1260–1266.

Can, A., Yalcin, M., Doğar, C., 2002. Electro coagulation of some reactive dyes: a statistical investigation of some electrochemical variables. Waste Manag. 22, 491–499.

Can, O.T., Kobya, M., Demirbas, E., Bayramoglu, M., 2006. Treatment of the textile wastewater by combined electro coagulation. Chemosphere 62, 181–187.

Dermontbouchard, Ma, X., isaacson, Carl, 2009. Colloidal properties of aqueous fullerenes: Iso electric points and aggregation kinetics of C60 and C60 derivatives. Environ. Sci. Technol. 43, 6597–6603.

Gurusamy Annadurai, S.S., Lee, D.J.S., 2004. Simultaneous removal of turbidity and humic acid from high turbidity stormwater. Adv. Environ. Res. 8, 713–725.

Holbrook, R.D., Mansfeld, C.B., Bott, C.B., 2015. Behavior and removal of multiwall carbon nanotubes during simulated drinking water treatment process. J. Environ. Eng. (submitted for publication).

Hyung, H., Kim, J.H., 2009. Dispersion of C60 in natural water and removal by conventional drinking water treatment processes. Water Res. 43 (9), 2463–2470.

Lin, D.H., Tian, X.L., Wu, F.C., Xing, B.S., 2010. Fate and transport of engineered nanomaterials in the environment. J. Environ. Qual. 39 (6), 1896–1908.

Liu, N., Liu, C.L., Zhang, J., Lin, D.H., 2012. Removal of dispersant-stabilized carbon nanotubes by regular coagulants. J. Environ. Sci. 24 (8), 1364–1370.

Luan, Z.K., Tan, H.X., 1992. Coagulation–flocculation characteristic sand mechanism of poly aluminum salts. Acta Sci. Circumstance 12 (2), 129–137.

Merzouk, B., Gourich, B., Sekki, A., Madani, K., Chibane, M., 2009. Removal turbidity and separation of heavy metals using electro coagulation–electroflotation technique a case study. J. Hazard. Mater. 164, 215–222.

Pan, B., Xing, B.S., Liu, W.X., Tao, S., Lin, X.M., Zhang, X.M., 2006. Distribution of sorbed phenanthrene and pyrene in different humic fractions of soils and importance of humic. Environ. Pollut. 143, 24–33.

Pinotti, A., Zaritzky, N., 2001. Effect of aluminum sulfate and cationic poly electrolytes on the destabilization of emulsified wastes. Waste Manag. 21 (6), 535–542.

Reijnders, L., 2006. Cleaner nanotechnology and hazard reduction of manufactured nanoparticles. J. Clean. Prod. 14 (2), 124–133.

Sparks, D.L., 2003. Environmental Soil Chemistry. second ed. Academic Press, pp. 271–273.

Wiesner, M.R., Lowry, G.V., Alvarez, P., Dionysiou, D., Biswas, P., 2006. Assessing the risks of manufactured nanomaterials. Environ. Sci. Technol. 40 (14), 4336–4345.

Zhang, Y., Chen, Y.S., Westerhoff, P., Hristovski, K., Crittenden, J.C., 2008. Stability of commercial metal oxide nanoparticles in water. Water Res. 42 (8-9), 2204–2212.

Zhang, L.Z., Zhao, Q., Wang, S.T., Mashayekhi, H., Li, Xin, Xing, B.S., 2014. Influence of ions on the coagulation and removal of fullerene in aqueous phase. Sci. Total Environ. (1), 466–467 (604-608).